



Published in final edited form as:

Stroke. 2008 May ; 39(5): 1569–1574. doi:10.1161/STROKEAHA.107.502047.

Dual-Modality Monitoring of Targeted Intraarterial Delivery of Mesenchymal Stem Cells After Transient Ischemia

Piotr Walczak, MD, Jian Zhang, MD, Assaf A. Gilad, PhD, Dorota A. Kedziorek, MD, Jesus Ruiz-Cabello, PhD, Randell G. Young, DVM, Mark F. Pittenger, PhD, Peter C.M. van Zijl, PhD, Judy Huang, MD, and Jeff W.M. Bulte, PhD

From the Neurosection, Division of MR Research, Russell H. Morgan Department of Radiology and Radiological Science (P.W., A.A.G., D.A.K., J.R.-C., P.C.M.v.Z., J.W.M.B.), the Cellular Imaging Section and Vascular Biology Program, Institute for Cell Engineering (P.W., A.A.G., D.A.K., J.R.-C., J.W.M.B.), the Departments of Neurosurgery (J.Z., J.H.), Chemical and Biomolecular Engineering (J.W.M.B.), and Biomedical Engineering (J.W.M.B.), The Johns Hopkins University School of Medicine, Baltimore, Md; Osiris Therapeutics Inc (R.G.Y., M.F.P.), Baltimore Md; and F.M. Kirby Center for Functional Brain Imaging (P.C.M.v.Z.), Kennedy Krieger Institute, Baltimore, Md.

Abstract

Background and Purpose—In animal models of stroke, functional improvement has been obtained after stem cell transplantation. Successful therapy depends largely on achieving a robust and targeted cell engraftment, with intraarterial (IA) injection being a potentially attractive route of administration. We assessed the suitability of laser Doppler flow (LDF) signal measurements and magnetic resonance (MR) imaging for noninvasive dual monitoring of targeted IA cell delivery.

Methods—Transient cerebral ischemia was induced in adult Wistar rats ($n = 25$) followed by IA or intravenous (IV) injection of mesenchymal stem cells (MSCs) labeled with superparamagnetic iron oxide. Cell infusion was monitored in real time with transcranial laser Doppler flowmetry while cellular delivery was assessed with MRI in vivo (4.7T) and ex vivo (9.4T).

Results—Successful delivery of magnetically labeled MSCs could be readily visualized with MRI after IA but not IV injection. IA stem cell injection during acute stroke resulted in a high variability of cerebral engraftment. The amount of LDF reduction during cell infusion (up to 80%) was found to correlate well with the degree of intracerebral engraftment, with low LDF values being associated with significant morbidity.

Conclusions—High cerebral engraftment rates are associated with impeded cerebral blood flow. Noninvasive dual-modality imaging enables monitoring of targeted cell delivery, and through interactive adjustment may improve the safety and efficacy of stem cell therapy.

Keywords

laser Doppler flow; MRI; stroke; stem cells; transplantation

© 2008 American Heart Association, Inc.

Correspondence to Jeff W.M. Bulte, PhD, Russell H. Morgan Dept. of Radiology and Radiological Science, Johns Hopkins University School of Medicine, 217 Traylor, 720 Rutland Ave, Baltimore, MD 21205-2195. jwmbulte@mri.jhu.edu.

Disclosures

Mark Pittenger and Randall Young own stock in Osiris Therapeutics.

Recent discoveries in the field of stem cell research have opened new avenues for the therapy of complex diseases, particularly those of the central nervous system. It has been shown repeatedly in animal models that neurological deficits can be diminished by the introduction of therapeutic cells.^{1,2} These observations in animal models provided the basis for the first clinical trials in Parkinson disease³ and stroke patients.^{4–6}

Stroke is a leading cause of serious, long-term disability, and survivors of ischemic insults have little effective treatment available. Although evidence of the beneficial effects of stem cells in animal stroke models is growing, the mechanisms behind the improvements are still unclear.⁷ Some investigators have postulated that functional improvement is related to trophic support, which promotes survival of challenged neurons in the penumbra,⁸ inducing myelination and neural plasticity,⁹ or is attributable to other factors, such as neoangiogenesis.¹⁰ Other researchers suggest that functional improvement is related to both neuronal differentiation and integration.¹¹ In any case, demonstration of therapeutic effects have been modest to date, and clearly, optimization of robust engraftment and detailed characterization of basic cellular events, such as migration, differentiation, and graft-host interactions, remains essential.

One obstacle that has hampered the advancement of stem cell transplantation is inadequate methodology to allow stem cell characterization in living organisms. Several techniques for noninvasive *in vivo* cellular imaging have been developed, including intravital multi-photon microscopy,^{12,13} bioluminescence,¹⁴ PET,¹⁵ and MRI.^{16–18} In stroke, MRI has been used in rats to demonstrate that embryonic stem cells¹⁹ or neural stem cells²⁰ grafted into the hemisphere contralateral to the ischemic lesion migrate along white matter tracts and populate the border zone of the ischemic brain lesion. MRI has also depicted migration of neural progenitors from the cisterna magna to the ischemic lesion.^{21,22}

Because of their relatively low immunogenicity and easy way of isolation, mesenchymal stem cells (MSCs) have recently gained interest as potential cell types for improvement of clinical outcome in neurodegenerative diseases, including stroke.^{5,23,24} However, the most optimal route of injection is at present unknown. Brain intraparenchymal injections can be targeted toward the lesion but are invasive, and multiple injections may be required to cover the entire area of the stroke lesion. Intracerebroventricular (ICV) injection of cells enables widespread cerebral engraftment of cells along the entire neuroaxis, but is limited for lesions located more remote from the ventricles. Intravenous (IV) injection is least invasive but may lead to low numbers of engrafted cells at the lesion and major trapping in the lung, liver, and spleen.^{25,26} Intraarterial (IA) injection, on the other hand, may be used to bypass the initial uptake by the systemic organs and deliver larger numbers of cells directly to the ischemic lesion, once vessels are reperfused. Clinical translation of any of these stem cell delivery strategies mandates the use of noninvasive monitoring techniques. In this study, we therefore investigated the feasibility of monitoring intraarterial cell delivery after transient ischemia with laser Doppler flow (LDF) measurements of cerebral blood flow in conjunction with MRI cell tracking.

Materials and Methods

Cell Culture and Labeling

MSCs derived from the bone marrow of adult Fisher 344 rats were isolated as previously described²⁷ and expanded *in vitro* using α -MEM/F12 medium containing 10% fetal bovine serum. Before transplantation, cells were magnetically labeled with Feridex (Berlex Imaging) mixed with the transfection agent poly-L-lysine (Sigma-Aldrich), added at 25 μ g Fe/mL to the cell cultures for a 24-hour incubation.²⁸ The iron content (pg Fe/cell) was determined using a Ferrozin-based spectrophotometric as previously described.²⁸

During expansion, cells were also labeled with BrdU (Invitrogen). Cells were subjected to 2 pulses of BrdU (2 hours of incubation each with 10 $\mu\text{mol/L}$ BrdU) performed on 2 consecutive days. Viability and proliferation rates of labeled cells were determined by trypan blue dye exclusion and MTS assay,¹⁷ respectively. For transplantation, labeled cells were suspended in phosphate-buffered saline (PBS) at a density of $1 \times 10^6/\text{mL}$.

MCAO, Cell Infusion, and LDF Measurements

All animal experiments were approved by our Institutional Animal Care and Use Committee. Adult (250 to 300 g) female Wistar rats ($n = 25$) were studied under isoflurane (1% to 2%) anesthesia. Transient focal cerebral ischemia was induced by 2-hour middle cerebral artery occlusion (MCAO) with an intraluminal suture.²⁹ Transcranial LDF measurements (Moor Instruments DRT4) were used to monitor the relative cerebral blood flow during the entire ischemia experiment, as well as throughout the injection period. To this end, a small area of the skull above the right corpus striatum was thinned with a drill for positioning of the fiber optic probe. LDF measurements were recorded starting before suture placement and continued throughout the ischemia and cell infusion procedures. After withdrawal of the suture and 30 minutes reperfusion, the extracranial right internal carotid artery (ICA) ipsilateral to the MCAO was cannulated with PE20 Intramedic polyethylene tubing (Clay Adams Inc). Cells were infused at 1 mL/min using a 27G needle; after 30 seconds, the injection was paused for 10 seconds and then reinitiated for another 30 seconds to complete the injection of a total of 1×10^6 cells. In control animals ($n = 4$), the same volume (1 mL) of phosphate-buffered saline was injected IA. For intravenous delivery ($n = 4$) 1×10^6 cells, suspended in 1 mL saline, were infused into the cannulated femoral vein.

MR Imaging

Isoflurane-anesthetized rats were horizontally immobilized in a custom-made probe, equipped with a 20-mm surface coil. In vivo imaging was performed using a Bruker 4.7T horizontal bore magnet. The in vivo imaging parameters were: (1) a T2-weighted 3D spin echo (SE) sequence with repetition time (TR) = 1300 ms, echo time (TE) = 98 ms, number of averages (NAV) = 2, field of view (FOV) = $34 \times 22 \times 11$ mm, matrix = $128 \times 64 \times 32$, and resolution = $266 \times 343 \times 350$ μm ; and (2) a 3D T2*-weighted gradient echo (GRE) sequence with TR = 300 ms, TE = 5 ms, NAV = 4, FOV = $10 \times 16 \times 4$ mm, matrix = $128 \times 128 \times 12$, and resolution = $83 \times 125 \times 333$ μm . The first imaging session was performed before the MCAO/cell infusion procedure, and the second was performed between 2 and 24 hours after the procedure. After in vivo MRI, animals were transcardially perfused with 0.1 mol/L PBS containing 4% paraformaldehyde, and the brains were removed for high-resolution ex vivo imaging and further histological analysis.

For ex vivo MRI, brains were placed in 20-mm NMR tubes filled with Fomblin LC08 (Ausimont USA Inc.)³⁰ and imaged using a Bruker 9.4 T horizontal bore magnet using a 3D GRE sequence with TR = 100 ms, TE = 5 ms, NAV = 4, FOV = $21 \times 16 \times 16$ mm, matrix = $256 \times 196 \times 196$, and an isotropic resolution of 85 μm . MRI data sets were processed with Amira 3.1 software (Mercury Computer Systems).

Histopathology

Brains were cryopreserved in 20% sucrose for 24 hours, and then sectioned at 20 μm using a cryostat. To determine the efficiency of cell labeling as well as to correlate the histopathology with MRI, tissue preparations were processed for Prussian blue²⁸ for Feridex iron and immunohistochemistry for BrdU (rat monoclonal antibody OBT0030, 1:400; Accurate Chemicals, as primary, and goat-anti rat 488, A11008, 1:300, Molecular Probes, as secondary). Microscopic analysis was performed using Olympus X51 and IX71

epifluorescence microscopes equipped with an Olympus DP-70 digital acquisition system. MRI data sets were processed with Amira 3.1 software (Mercury Computer Systems).

Results

Cell Labeling

Magnetic cell labeling of MSCs was highly efficient, with nearly all cells being labeled. Prussian blue staining (Figure 1A) demonstrated numerous iron-containing vesicles throughout the cellular cytoplasm. The average amount of Feridex labeling was 15 to 20 pg of iron per cell. After BrdU pulsing before transplantation, the colabel BrdU was detected immunohistochemically in the majority of the MSCs (Figure 1B). On average, approximately 10% of cells were found to be nondividing. The viability (>95%) rate was similar for labeled and unlabeled cells. The MTS assay demonstrated minimal changes after Feridex labeling, with proliferation values $\geq 90\%$ that of unlabeled cells at 24 hours after labeling.

LDF Monitoring of Cell Delivery

Intraluminal occlusion of MCAO resulted in a consistent reduction of CBF to about 30% of baseline (Figure 2). This level was maintained throughout a 2-hour period in all animals tested. After removal of the suture and reperfusion, CBF returned to near-baseline levels. The delivery of 1×10^6 MSCs into the carotid artery ipsilateral to the ischemic lesion was initiated 30 minutes into the reperfusion period, and resulted in a high variability of cell engraftment. In 3 animals (17%), there was no change in LDF signal (Figure 2, black line) with no cells detectable in the brain by MRI (Figure 3a and 3b) and histology (results not shown). In 8 animals (47%), the LDF signal drop was moderate (10% to 30%; Figure 2, blue line), with moderate cell engraftment (Figure 3c and 3d). In 6 animals (35%), the injection caused a significant (80% to 90%) reduction in LDF signal (Figure 2, red line) and a rapid death within 2 to 4 hours in 4 animals. Although the MCAO procedure itself can lead to a high mortality we observed, that in control, nontransplanted animals that underwent MCAO the mortality during the first 48 hours was about 7% as compared to 67% in the MCAO-cell transplant group.

MR Monitoring of Targeted Cell Delivery

In vivo T2*-weighted MRI (Figure 3c and 3e) detected the engraftment of labeled cells within the right ICA vascular territory, as represented by the presence of strong signal voids, which was further confirmed by high-resolution ex vivo MRI (Figure 3d and 3f). Engraftment of injected MSCs was found to occur primarily throughout the right ICA vascular territory and only occasionally in the contralateral hemisphere (Figure 3c through 3g), indicating that cells engrafted during the first pass without systemic circulation. These findings were further confirmed by Prussian blue staining and immunofluorescent anti-BrdU microscopy (Figure 4a and 4b). One day after cell infusion, iron and BrdU-positive cells were located within the cerebral capillary bed (Figure 4a and 4b). At later time points (10 days after transplantation), BrdU-positive cells were found to have entered the parenchyma of the cerebral cortex (Figure 4c). In contrast to the IA cell delivery, IV injection resulted in undetectable MRI levels of cell engraftment (Figure 3g), with very few cells present in the brain after histological evaluation. While the amount of iron within labeled MSCs generated sufficient contrast for cell detection on T2*-weighted MR images (with a T2* sequence being the most sensitive to magnetic field disturbances caused by iron-labeled cells), T2-weighted imaging (less sensitive to iron) allowed a proper visualization of the ischemic brain tissue (Figure 5).

Discussion

We have demonstrated that IA infusion of MSCs in rats during the acute stage of stroke results in a high variability of targeted cellular delivery in the brain. The results of our study suggest that monitoring of cell delivery and engraftment is possible using both LDF measurements and MRI.

Evidence for a positive outcome of cell-based therapies is now mounting in animal stroke models.^{2,22,31} For instance, bone marrow–derived mesenchymal cells implanted 24 hours after MCAO in rats led to behavioral improvements, and grafted cells were detected throughout the middle cerebral artery (MCA) territory up to 2 weeks after grafting.³² In a similar experiment, grafted mesenchymal cells led to functional improvements that mediated remyelination and synaptic plasticity enhancement.⁹ Initial clinical trials of therapeutic IA stem cell transplantation have now been performed. In stroke patients, autologous bone marrow–derived mononuclear cells were infused into the MCA ipsilateral to the stroke lesion.⁶

Now that clinical trials are being performed in stroke patients,^{4,6} it is of key importance to design and establish safe and efficient methods to deliver cells to the sites of ischemic brain damage. Among the available routes for intracerebral cell delivery are intraparenchymal,^{19,20,33} ICV,²² IV,³⁴ and IA.³² Intraparenchymal, stereotactic cell injection is based on insertion of a needle and infusion of the cells into the brain parenchyma. Although this method provides precision with regard to the graft placement and there is some evidence on directed cell migration toward the ischemic site,¹³ there is usually a poor cell distribution throughout the lesion,³⁵ as a result of the limited migratory potential of cells in the adult brain.³⁶ Inadequate cell migration can be addressed by performing multiple injections; however, this in turn enhances the risk of brain injury and can lead to nonuniform cell distribution with the risk of graft malfunction.³⁷ In contrast, IV delivery is a relatively easy and noninvasive procedure, allowing a broad distribution of cells, and enabling exposure of cells to chemoattractant signals (originating from the lesion) that can selectively accumulate them within the target tissue. However, IV injection leads to an initial random dispersion of cells throughout the body, with cells accumulating in trapping and filtering organs such as the lungs, liver, and spleen.^{25,26} Only a small amount of cells may be able to reach the target brain lesion, and thus, the cell dose must be appropriately adjusted. Indeed, when we performed IV injections, we could only detect trace quantities of cells within the brain on histology; the low levels of engrafted cells could not be detected by MRI. The advantage of ICV injection is that cells have access to a larger surface of the brain,²² although the success of this approach depends even more on the robust migratory properties of grafted cells, their appropriate navigation while in the CSF, and on crossing the blood-CSF barrier with subsequent penetration into the parenchyma. In addition, access to the ventricular system in humans is highly invasive and requires drilling a hole in the skull for placement of a ventriculostomy catheter.

In contrast, IA cell delivery provides the opportunity to target the entire ischemic lesion within the relevant vascular territory after transient ischemia. Furthermore, IA delivery of therapeutic cells into the brain is clinically relevant, because percutaneous transfemoral catheterization of selected intracranial arteries using microcatheters is already commonly used in clinical practice.^{38,39}

Cerebral ischemia results from transient or permanent vascular occlusions; in the case of a transient occlusion cells may be targeted toward the entire lesion. However, in the case of a permanent occlusion they will be distributed only throughout the penumbra region.

The mechanisms regulating intracerebral engraftment of infused stem cells are complex and depend on the physical and biological properties of both the transplanted cells and blood vessels. The rheological component is affected by the ratio of the cell diameter to the capillary size. These dimensional disproportions may be further convoluted by cerebral edema after stroke. The results from this study show that cells as large as 20 to 50 μm (range of mesenchymal cell diameter) are able to bypass the intracerebral entrapment and remain within the systemic vasculature in 17% of animals (Figure 3a). In our study, MSCs were infused into the ipsilateral carotid artery at the completion of the 2-hour ischemic period. The typical MCAO rat model, similar to human stroke, may evolve with significant variability with regard to stroke size, location, and symptom severity. One conceivable explanation for the broad variance in cerebral engraftment in our study is that each individual animal demonstrated a heterogenous timing and pattern of pathophysiological changes. For the animals with no engraftment (Figure 3a and 3b), cell delivery may have been completed before a sufficient cascade of ischemia-related changes occurred to allow subsequent cell engraftment. In the animals with moderate engraftment, recruitment forces were sufficient to attract and anchor a fraction of the grafted cells within the cerebral microvessels, whereas in the high engraftment group, these chemoattractant forces, and possibly other factors such as brain edema, caused excessive cell accumulation and compromised microvascular circulation. In the latter group, cells were rarely found to have entered the other hemisphere, indicating near complete trapping; in the moderate engraftment group, however, a substantial proportion of cells was able to cross into the other hemisphere.

In conclusion, IA delivery of stem cells offers the advantage of directly targeting the damaged tissue, and circumvents the problem of cell trapping in filtering organs such as the lung, liver, or spleen. However, it needs to be emphasized that the IA delivery represents a paradox, as the goal is to achieve a high cellular engraftment without inducing microvascular occlusions and compromising cerebral blood flow. In this article we have demonstrated that despite the benefits of intraarterial delivery of stem cells to the ischemic brain, there is a clear risk of vascular occlusion. Thus, noninvasive monitoring methods as described in this study are mandatory for possible clinical translation of IA stem cell delivery in stroke patients.

Acknowledgments

We are grateful to Dr Miroslaw Janowski for his valuable input and to Mary McAllister for editorial assistance.

Sources of Funding

This work was supported by NIH RO1 NS045062 and a grant from Osiris Therapeutics Inc.

References

1. Bjorklund A, Stenevi U. Reconstruction of the nigrostriatal dopamine pathway by intracerebral nigral transplants. *Brain Res* 1979;177:555–560. [PubMed: 574053]
2. Borlongan CV, Tajima Y, Trojanowski JQ, Lee VM, Sanberg PR. Transplantation of cryopreserved human embryonal carcinoma-derived neurons (nt2n cells) promotes functional recovery in ischemic rats. *Exp Neurol* 1998;149:310–321. [PubMed: 9500961]
3. Kordower JH, Freeman TB, Snow BJ, Vingerhoets FJ, Mufson EJ, Sanberg PR, Hauser RA, Smith DA, Nauert GM, Perl DP, Olanow CW. Neuropathological evidence of graft survival and striatal reinnervation after the transplantation of fetal mesencephalic tissue in a patient with parkinson's disease. *N Engl J Med* 1995;332:1118–1124. [PubMed: 7700284]

4. Kondziolka D, Wechsler L, Goldstein S, Meltzer C, Thulborn KR, Gebel J, Jannetta P, DeCesare S, Elder EM, McGrogan M, Reitman MA, Bynum L. Transplantation of cultured human neuronal cells for patients with stroke. *Neurology* 2000;55:565–569. [PubMed: 10953194]
5. Bang OY, Lee JS, Lee PH, Lee G. Autologous mesenchymal stem cell transplantation in stroke patients. *Ann Neurol* 2005;57:874–882. [PubMed: 15929052]
6. de Freitas GR, Mendonca MLF, Bezerra DC, Silva SA, Falcao CH, Gonzales CS, Moreira RC, Haddad AF, Tucho FA, Santos DP, Andre C, Mesquita CT, Oliveira AA, Elia V, Dohmann HJ, Borojevic R, Mendez-Otero R, Dohmann H. Safety and feasibility of intra-arterial autologous bone marrow mononuclear cell transplantation in acute ischemic stroke. *Stroke* 2006;37:624–625.
7. Lindvall O, Kokaia Z. Stem cell therapy for human brain disorders. *Kidney Int* 2005;68:1937–1939. [PubMed: 16221169]
8. Ourednik J, Ourednik V. Graft-induced plasticity in the mammalian host CNS. *Cell Transplant* 2004;13:307–318. [PubMed: 15191168]
9. Shen LH, Li Y, Chen J, Zhang J, Vanguri P, Borneman J, Chopp M. Intracarotid transplantation of bone marrow stromal cells increases axon-myelin remodeling after stroke. *Neuroscience* 2006;137:393–399. [PubMed: 16298076]
10. Hess DC, Hill WD, Martin-Studdard A, Carroll J, Brailer J, Carothers J. Bone marrow as a source of endothelial cells and neuron-expressing cells after stroke. *Stroke* 2002;33:1362–1368. [PubMed: 11988616]
11. Chen J, Li Y, Wang L, Lu M, Zhang X, Chopp M. Therapeutic benefit of intracerebral transplantation of bone marrow stromal cells after cerebral ischemia in rats. *J Neurol Sci* 2001;189:49–57. [PubMed: 11535233]
12. Haydar TF, Ang E Jr, Rakic P. Mitotic spindle rotation and mode of cell division in the developing telencephalon. *Proc Natl Acad Sci U S A* 2003;100:2890–2895. [PubMed: 12589023]
13. Tran-Dinh A, Kubis N, Tomita Y, Karaszewski B, Calando Y, Oudina K, Petite H, Seylaz J, Pinard E. In vivo imaging with cellular resolution of bone marrow cells transplanted into the ischemic brain of a mouse. *Neuroimage* 2006;31:958–967. [PubMed: 16516498]
14. Tang Y, Shah K, Messerli SM, Snyder E, Breakefield X, Weissleder R. In vivo tracking of neural progenitor cell migration to glioblastomas. *Hum Gene Ther* 2003;14:1247–1254. [PubMed: 12952596]
15. Adonai N, Nguyen KN, Walsh J, Iyer M, Toyokuni T, Phelps ME, McCarthy T, McCarthy DW, Gambhir SS. Ex vivo cell labeling with ⁶⁴Cu-pyruvaldehyde-bis(n4-methylthiosemicarbazone) for imaging cell trafficking in mice with positron-emission tomography. *Proc Natl Acad Sci U S A* 2002;99:3030–3035. [PubMed: 11867752]
16. Bulte JW, Douglas T, Witwer B, Zhang SC, Strable E, Lewis BK, Zywicke H, Miller B, van Gelderen P, Moskowitz BM, Duncan ID, Frank JA. Magnetodendrimers allow endosomal magnetic labeling and in vivo tracking of stem cells. *Nat Biotechnol* 2001;19:1141–1147. [PubMed: 11731783]
17. Walczak P, Kedziorek DA, Gilad AA, Lin S, Bulte JW. Instant MR labeling of stem cells using magnetoelectroporation. *Magn Reson Med* 2005;54:769–774. [PubMed: 16161115]
18. Bulte JW, Duncan ID, Frank JA. In vivo magnetic resonance tracking of magnetically labeled cells after transplantation. *J Cereb Blood Flow Metab* 2002;22:899–907. [PubMed: 12172375]
19. Hoehn M, Kustermann E, Blunk J, Wiedermann D, Trapp T, Wecker S, Focking M, Arnold H, Hescheler J, Fleischmann BK, Schwandt W, Buhrle C. Monitoring of implanted stem cell migration in vivo: A highly resolved in vivo magnetic resonance imaging investigation of experimental stroke in rat. *Proc Natl Acad Sci U S A* 2002;99:16267–16272. [PubMed: 12444255]
20. Modo M, Mellodew K, Cash D, Fraser SE, Meade TJ, Price J, Williams SC. Mapping transplanted stem cell migration after a stroke: A serial, in vivo magnetic resonance imaging study. *Neuroimage* 2004;21:311–317. [PubMed: 14741669]
21. Zhang ZG, Jiang Q, Zhang R, Zhang L, Wang L, Arniago P, Ho KL, Chopp M. Magnetic resonance imaging and neurosphere therapy of stroke in rat. *Annals of Neurology* 2003;53:259–263. [PubMed: 12557295]
22. Jiang Q, Zhang ZG, Ding GL, Zhang L, Ewing JR, Wang L, Zhang R, Li L, Lu M, Meng H, Arbab AS, Hu J, Li QJ, Pourabdollah Nejad DS, Athiraman H, Chopp M. Investigation of neural

- progenitor cell induced angiogenesis after embolic stroke in rat using mri. *Neuroimage* 2005;28:698–707. [PubMed: 16112879]
23. Chen J, Li Y, Katakowski M, Chen X, Wang L, Lu D, Lu M, Gautam SC, Chopp M. Intravenous bone marrow stromal cell therapy reduces apoptosis and promotes endogenous cell proliferation after stroke in female rat. *J Neurosci Res* 2003;73:778–786. [PubMed: 12949903]
 24. Nomura T, Honmou O, Harada K, Houkin K, Hamada H, Kocsis JDIV. Infusion of brain-derived neurotrophic factor gene-modified human mesenchymal stem cells protects against injury in a cerebral ischemia model in adult rat. *Neuroscience* 2005;136:161–169. [PubMed: 16229956]
 25. Kraitchman DL, Tatsumi M, Gilson WD, Ishimori T, Kedziorek D, Walczak P, Segars WP, Chen HH, Fritzsche D, Izbudak I, Young RG, Marcelino M, Pittenger MF, Solaiyappan M, Boston RC, Tsui BM, Wahl RL, Bulte JW. Dynamic imaging of allogeneic mesenchymal stem cells trafficking to myocardial infarction. *Circulation* 2005;112:1451–1461. [PubMed: 16129797]
 26. Hauger O, Frost EE, van Heeswijk R, Deminiere C, Xue R, Delmas Y, Combe C, Moonen CT, Grenier N, Bulte JW. MR evaluation of the glomerular homing of magnetically labeled mesenchymal stem cells in a rat model of nephropathy. *Radiology* 2006;238:200–210. [PubMed: 16373768]
 27. Pittenger MF, Mackay AM, Beck SC, Jaiswal RK, Douglas R, Mosca JD, Moorman MA, Simonetti DW, Craig S, Marshak DR. Multilineage potential of adult human mesenchymal stem cells. *Science* 1999;284:143–147. [PubMed: 10102814]
 28. Bulte JW, Arbab AS, Douglas T, Frank JA. Preparation of magnetically labeled cells for cell tracking by magnetic resonance imaging. *Methods Enzymol* 2004;386:275–299. [PubMed: 15120257]
 29. Belayev L, Alonso OF, Busto R, Zhao W, Ginsberg MD. Middle cerebral artery occlusion in the rat by intraluminal suture. Neurological and pathological evaluation of an improved model. *Stroke* 1996;27:1616–1622. discussion 1623. [PubMed: 8784138]
 30. Bulte JW, Zhang S, van Gelderen P, Herynek V, Jordan EK, Duncan ID, Frank JA. Neurotransplantation of magnetically labeled oligodendrocyte progenitors: Magnetic resonance tracking of cell migration and myelination. *Proc Natl Acad Sci U S A* 1999;96:15256–15261. [PubMed: 10611372]
 31. Willing AE, Lixian J, Milliken M, Poulos S, Zigova T, Song S, Hart C, Sanchez-Ramos J, Sanberg PR. Intravenous versus intrastriatal cord blood administration in a rodent model of stroke. *J Neurosci Res* 2003;73:296–307. [PubMed: 12868063]
 32. Li Y, Chen J, Wang L, Lu M, Chopp M. Treatment of stroke in rat with intracarotid administration of marrow stromal cells. *Neurology* 2001;56:1666–1672. [PubMed: 11425931]
 33. Walczak P, Chen N, Hudson JE, Willing AE, Garbuzova-Davis SN, Song S, Sanberg PR, Sanchez-Ramos J, Bickford PC, Zigova T. Do hematopoietic cells exposed to a neurogenic environment mimic properties of endogenous neural precursors? *J Neurosci Res* 2004;76:244–254. [PubMed: 15048922]
 34. Willing AE, Vendrame M, Mallery J, Cassady CJ, Davis CD, Sanchez-Ramos J, Sanberg PR. Mobilized peripheral blood cells administered intravenously produce functional recovery in stroke. *Cell Transplant* 2003;12:449–454. [PubMed: 12911133]
 35. Li Y, Chopp M, Chen J, Wang L, Gautam SC, Xu YX, Zhang Z. Intrastriatal transplantation of bone marrow nonhematopoietic cells improves functional recovery after stroke in adult mice. *J Cereb Blood Flow Metab* 2000;20:1311–1319. [PubMed: 10994853]
 36. O’Leary MT, Blakemore WF. Oligodendrocyte precursors survive poorly and do not migrate following transplantation into the normal adult central nervous system. *J Neurosci Res* 1997;48:159–167. [PubMed: 9130144]
 37. Olanow CW, Goetz CG, Kordower JH, Stoessl AJ, Sossi V, Brin MF, Shannon KM, Nauert GM, Perl DP, Godbold J, Freeman TB. A double-blind controlled trial of bilateral fetal nigral transplantation in Parkinson’s disease. *Ann Neurol* 2003;54:403–414. [PubMed: 12953276]
 38. Criado FJ, Lingelbach JM, Ledesma DF, Lucas PR. Carotid artery stenting in a vascular surgery practice. *J Vasc Surg* 2002;35:430–434. [PubMed: 11877688]

39. Higashida RT, Halbach VV, Dowd CF, Barnwell SL, Hieshima GB. Intracranial aneurysms: Interventional neurovascular treatment with detachable balloons—results in 215 cases. *Radiology* 1991;178:663–670. [PubMed: 1994399]

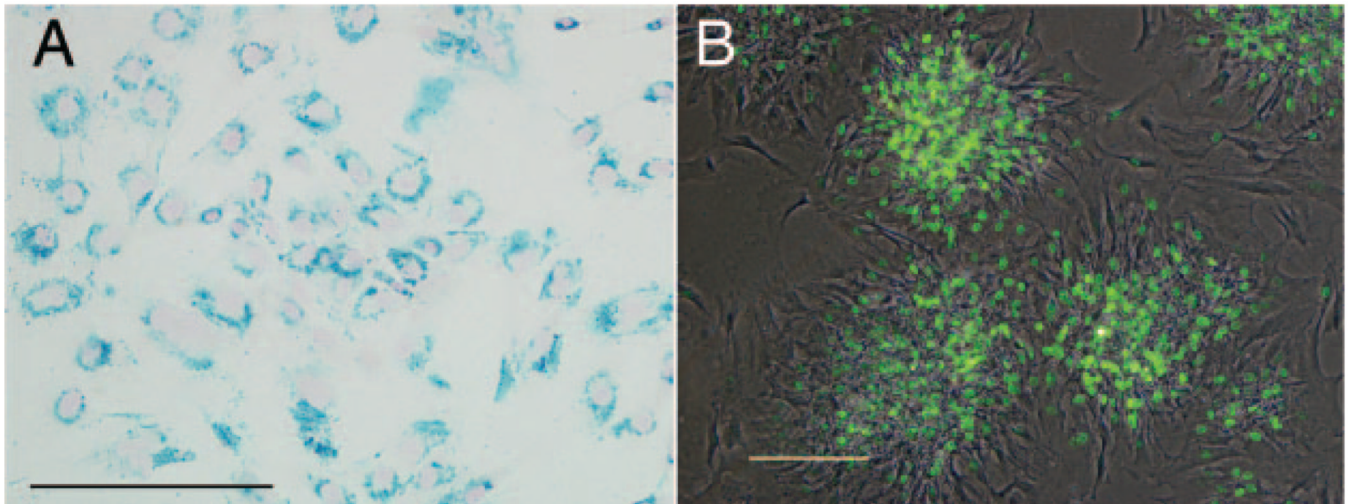


Figure 1.

In vitro characterization of labeled rat MSCs. A, Prussian blue staining of magnetically labeled cells. Nearly 100% of the cells are efficiently labeled with a characteristic perinuclear, endosomal distribution of the Feridex iron (blue precipitate). B, Fluorescent photomicrograph of anti-BrdU immunostaining, merged with phase-contrast image. BrdU-positive nuclei (green) are indicative of proliferative cells in the form of colonies, whereas peripheral cells are nondividing. Scale bars in A and B equal 200 μm .

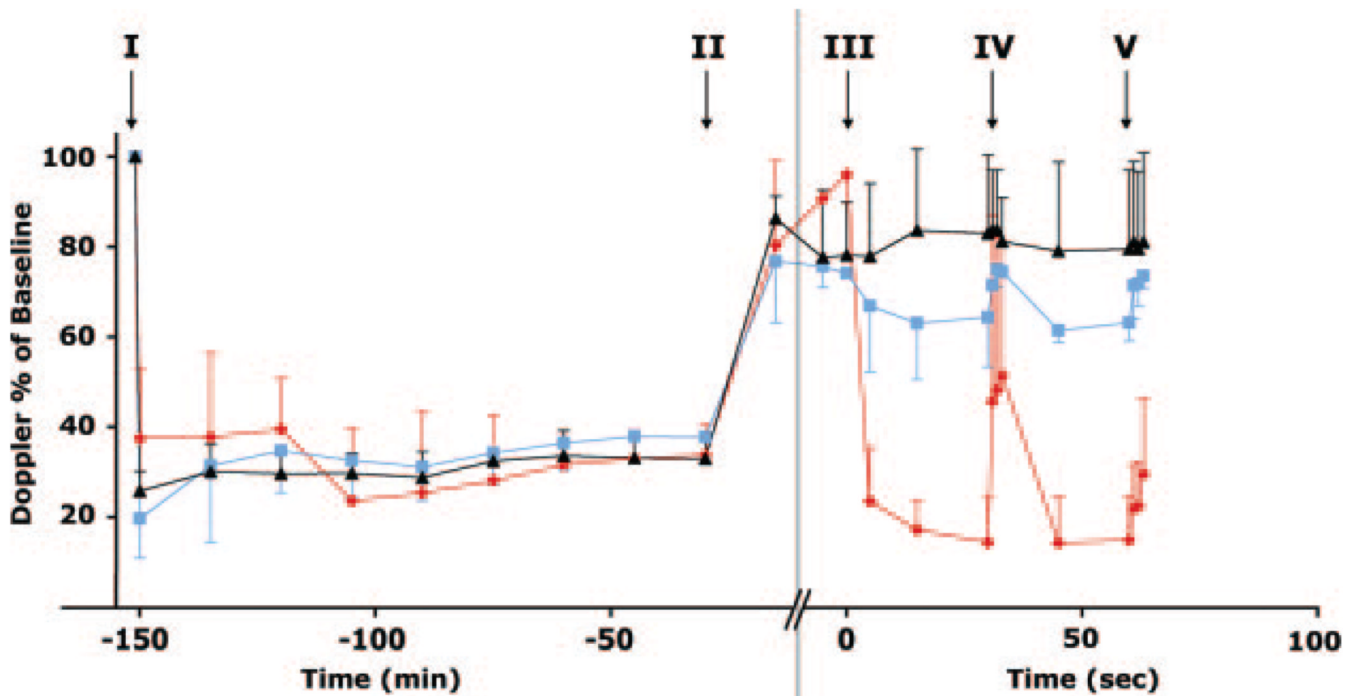


Figure 2.

LDF measurements of cerebral blood flow during ischemia induction and IA cell delivery compared to baseline values. Intraluminal occlusion of MCA initiated 150 minutes before cell infusion (I) resulted in a rapid and dramatic drop in LDF signal to 20% to 40% of baseline values which was maintained throughout the 2-hour ischemia period. After induction of ischemia, the occluding suture was removed, resulting in a quick restoration of cerebral blood flow (II). After intracarotid infusion of MSCs (III), the LDF signal decreases proportional to the intracapillary lodging of stem cells as detected by MRI (red - high engraftment; blue - moderate engraftment; black - no engraftment). The initial drop of LDF signal could be partially reversed when cell infusion was interrupted for 10 seconds (IV). A similar but variable restoration of LDF was observed at the completion of cell infusion (V). Whereas a reduction of LDF signal up to 50% did not seem to affect morbidity attributable to the intraarterial injection procedure (black and blue lines), a further reduction of cerebral blood flow was usually fatal (red line). The black, blue, and red lines represent mean \pm SD for $n = 3$, $n = 8$, and $n = 6$ of animals, respectively.

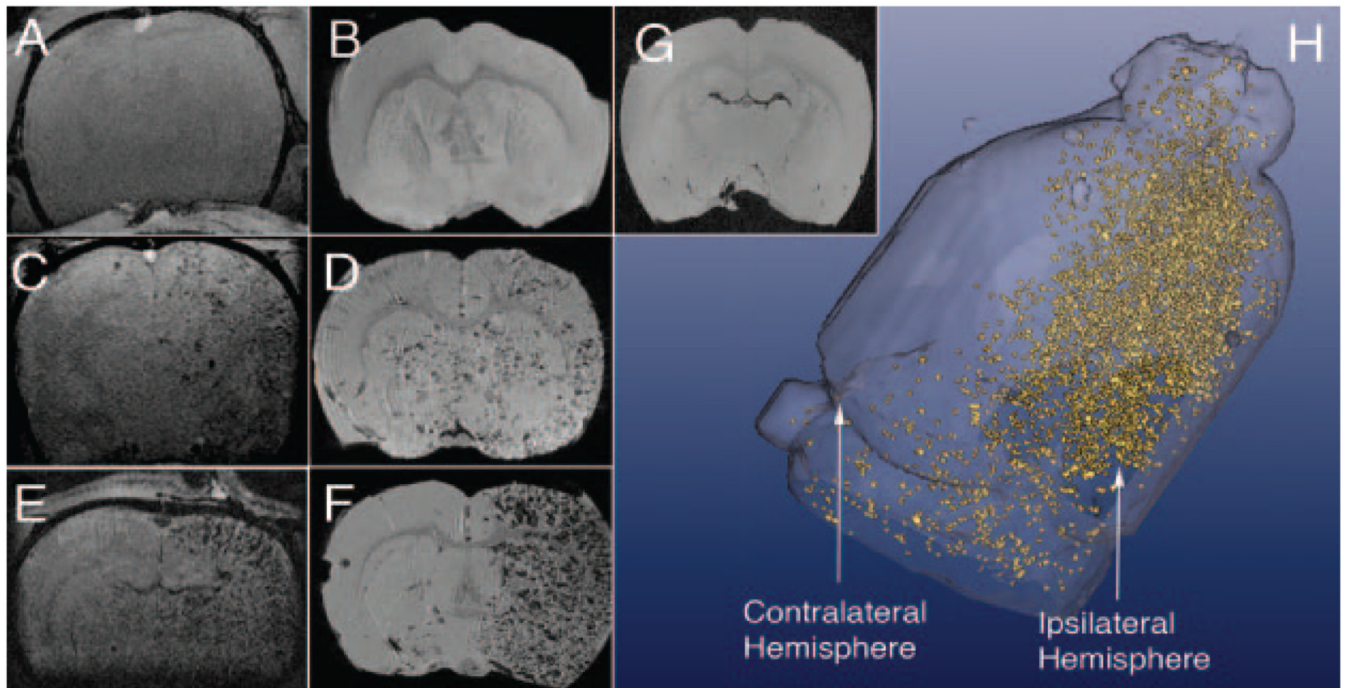


Figure 3.

MR images of intracerebral cell engraftment after IA (A–F, H) and IV (G) injection. MSCs appear as hypointense spots on T2*- weighted images. A, In vivo and (B) ex vivo MR images of an animal corresponding to the black line in Figure 2. No brain engraftment can be observed. In vivo (C) and ex vivo (D) MR images of an animal corresponding to the blue line in Figure 2. A moderate brain engraftment can be seen with some cells entering the other hemisphere. In vivo (E) and ex vivo (F) MR images of an animal corresponding to the red line in Figure 2. A massive engraftment can be observed, but the cell distribution is limited to the right hemisphere perfused by the right carotid artery used for injection. G, No engraftment could be detected after IV injection. H, 3D reconstruction of cellular distribution in the brain of example shown in E and F. Cells distributed widely throughout the right brain hemisphere, with a prevalence for the area directly fed by the right internal carotid artery; the territory of the anterior and posterior cerebral arteries also exhibit significant engraftment. Very few cells were detected in the contralateral (left) hemisphere, suggesting that cells did not circulate systemically before arriving at their final location.

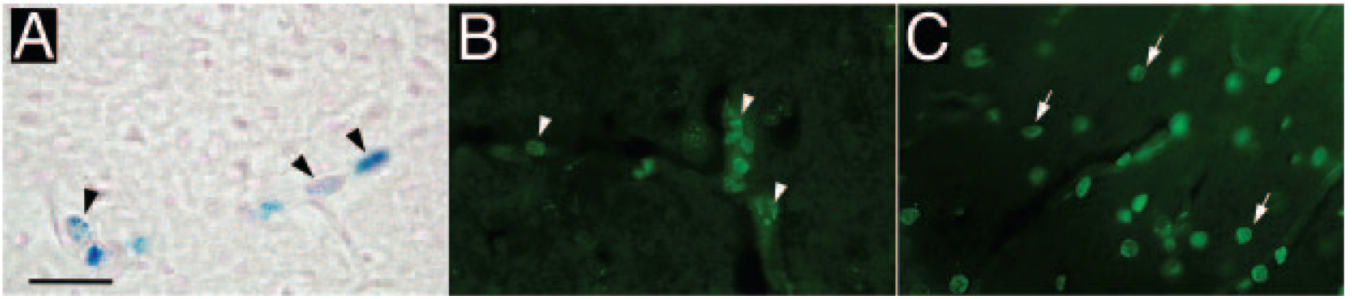


Figure 4. Histopathologic detection of engrafted MSCs. Prussian blue staining (A) and immunohistochemistry anti-BrdU (B) at early time points (1 day) demonstrate single cells found within the capillaries (arrow heads) throughout the ipsilateral brain hemisphere. Ten days after transplantation BrdU-positive cells were found within the brain parenchyma, indicating active migration across vessel walls (C, arrows). Scale bar = 40 μ m.

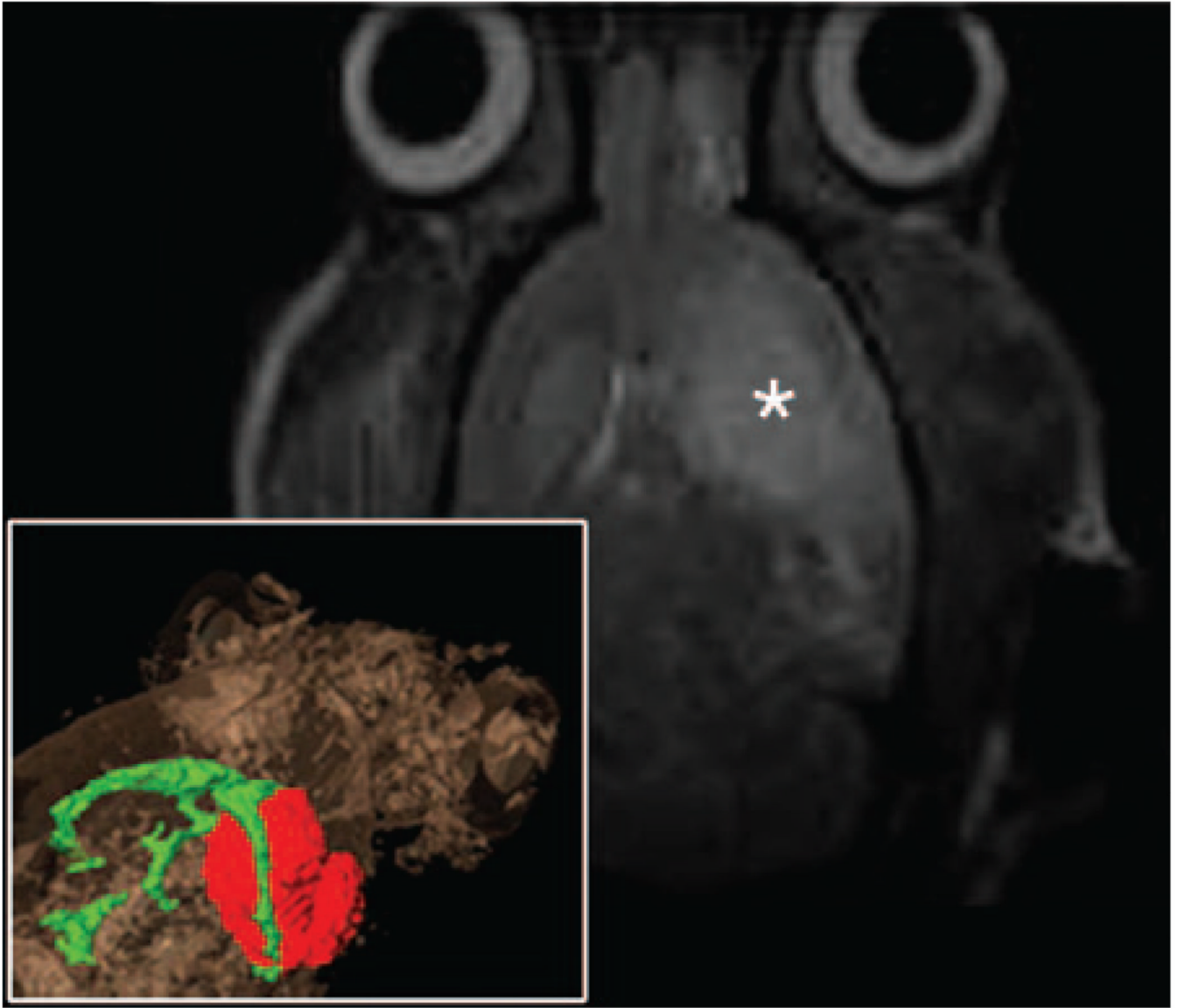


Figure 5. T2-weighted MRI 24 hours after Feridex-labeled MSC injection. The presence of the cellular contrast agent does not hamper the detection of the ischemic lesion (asterisk). Inset shows 3D reconstruction with the area of ischemia in red and the ventricular system in green.